Neuropharmacology 65 (2013) 143–155

Contents lists available at SciVerse ScienceDirect

Neuropharmacology

journal homepage: www.elsevier.com/locate/neuropharm

NMDA receptor blockade impairs the muscarinic conversion of sub-threshold transient depression into long-lasting LTD in the hippocampus–prefrontal cortex pathway *in vivo*: Correlation with gamma oscillations

Cleiton Lopes-Aguiar [a], Lezio Soares Bueno-Junior [a], Rafael Naime Ruggiero [a], Rodrigo Neves Romcy-Pereira [a,b,*], João Pereira Leite [a]

[a] Department of Neuroscience and Behavioral Science, Ribeirão Preto School of Medicine, University of São Paulo, Ribeirão Preto, São Paulo, Brazil
[b] Brain Institute, Federal University of Rio Grande do Norte (UFRN), Brazil

ARTICLE INFO

Article history:
Received 26 September 2011
Received in revised form
19 July 2012
Accepted 16 September 2012

Keywords:
Muscarinic neurotransmission
NMDA
Hippocampus
Prefrontal cortex
Long-term depression (LTD)
Synaptic Plasticity

ABSTRACT

Cholinergic fibers from the brainstem and basal forebrain innervate the medial prefrontal cortex (mPFC) modulating neuronal activity and synaptic plasticity responses to hippocampal inputs. Here, we investigated the muscarinic and glutamatergic modulation of long-term depression (LTD) in the intact projections from CA1 to mPFC *in vivo*. Cortical-evoked responses were recorded in urethane-anesthetized rats for 30 min during baseline and 4 h following LTD. In order to test the potentiating effects of pilocarpine (PILO), independent groups of rats received either a microinjection of PILO (40 nmol; i.c.v.) or vehicle, immediately before or 20 min after a sub-threshold LTD protocol (600 pulses, 1 Hz; LFS600). Other groups received either an infusion of the selective NMDA receptor antagonist (AP7; 10 nmol; intra-mPFC) or vehicle, 10 min prior to PILO preceding LFS600, or prior to a supra-threshold LTD protocol (900 pulses, 1 Hz; LFS900). Our results show that PILO converts a transient cortical depression induced by LFS600 into a robust LTD, stable for at least 4 h. When applied after LFS600, PILO does not change either mPFC basal neurotransmission or late LTD. Our data also indicate that NMDA receptor pre-activation is essential to the muscarinic enhancement of mPFC synaptic depression, since AP7 micro-injection into the mPFC blocked the conversion of transient depression into long-lasting LTD produced by PILO. In addition, AP7 effectively blocked the long-lasting LTD induced by LFS900. Therefore, our findings suggest that the glutamatergic co-activation of prefrontal neurons is important for the effects of PILO on mPFC synaptic depression, which could play an important role in the control of executive and emotional functions.

1. Introduction

Behavioral flexibility in mammals can be explained, at least in part, by the ability of their cortical circuits to undergo N-methyl-D-aspartate receptor (NMDAR)-dependent long-term potentiation (LTP) and depression (LTD) (Bear and Kirkwood, 1993; Buonomano and Merzenich, 1998; Feldman, 2009; Jones et al., 1999; Martin and Morris, 2002). In circuits connecting the hippocampus to the cortex, changes in synaptic efficacy conveyed by LTP and LTD are thought to be basic intercellular mechanisms for the acquisition, consolidation and retrieval of memory traces required during behavioral planning and execution (Bliss and Collingridge, 1993; Griffiths et al., 2008; Kemp and Manahan-Vaughan, 2007; Massey and Bashir, 2007; Warburton et al., 2003; Winocur et al., 2010). Moreover, the existence of a dynamic regulation of bidirectional plasticity at the synapse allows the control of information transfer and cortical processing of hippocampal inputs.

The medial prefrontal cortex (mPFC) is known to integrate information from the hippocampus, amygdala and several sub-cortical areas during tasks requiring working memory, behavioral inhibition and attention (Dalley et al., 2004; Goldman-Rakic, 1995a,b; Otani, 2003; Uylings et al., 2003; Vertes, 2006). Particularly, hippocampal afferents to the mPFC originate from the temporal region of CA1 and subiculum sending direct monosynaptic excitatory projections to pyramidal neurons in the dorsal and ventral divisions of the mPFC – prelimbic and infralimbic (Jay et al., 1989; Swanson, 1981; Thierry et al., 2000). In the prelimbic

* Corresponding author. Brain Institute, Federal University of Rio Grande do Norte (UFRN), 59056-450 Natal, RN, Brazil. Tel.: +55 84 8852 1551.
E-mail addresses: rnrpereira@gmail.com, rnrpereira@neuro.ufrn.br (R.N. Romcy-Pereira).

0028-3908/$ – see front matter © 2012 Elsevier Ltd. All rights reserved.
http://dx.doi.org/10.1016/j.neuropharm.2012.09.013

region, hippocampal synapses can express a long-lasting NMDAR-dependent LTP, as well as, a stable form of LTD, thought to be important for cognitive and affective functions of the mPFC (Floresco et al., 1997; Jay et al., 1995; Laroche et al., 2000, 1990; Takita et al., 1999). Both forms of synaptic plasticity are modulated by a variety of neurotransmitters and behavioral tasks (Garcia et al., 2008; Jay et al., 2004; Ohashi et al., 2003; Rocher et al., 2004; Wang and Yuan, 2009; Wierzynski et al., 2009). In particular, septo-hippocampal projections and afferents from the basal forebrain to the neocortex comprise an important modulator of cognition, with neurons in these areas showing increased firing rates during tasks of attention shifting and rapid-eye movement (REM) sleep (Gu, 2003; Hasselmo, 2006; Lucas-Meunier et al., 2003).

We have recently shown that short-term REM sleep deprivation impairs the late-phase maintenance of LTP in the dentate gyrus of the hippocampus, whereas it potentiates LTP maintenance in the mPFC, suggesting a differential regulation of hippocampal and cortical plasticity by the cholinergic system during sleep (Romcy-Pereira and Pavlides, 2004). In addition, muscarinic neurotransmission enhances the late-phase LTP without affecting induction or early LTP *in vivo*, which could promote long-lasting synaptic changes in the cortex, potentially enhancing mPFC-dependent memories (Lopes Aguiar et al., 2008). In order to investigate the effects of muscarinic receptor activation on prefrontal synaptic depression, we studied the modulatory effect of pilocarpine on sub-threshold transient depression of fPSPs in the hippocampal-prefrontal projections, and analyzed its interactions with the glutamatergic NMDA transmission *in vivo*.

2. Material and methods

2.1. Subjects

Seventy-five adult male Wistar rats (250–450 g) were housed in standard rodent cages in a colony room maintained at 24 °C under a 12 h light–12 h dark cycle with free access to food and water. All procedures were performed according to the Brazilian Council for the Control of Animal Experimentation (CONCEA) guidelines for animal research and approved by the ethics committee at the University of São Paulo. These guidelines abide by the National Institute of Health rules for the care and use of Laboratory animals (NIH Publications No. 8023, revised 1978). Experiments were designed to minimize the number of animals used and their suffering.

2.2. Surgery and electrophysiology setup

Rats were anesthetized with urethane (1.2–1.5 g/kg, i.p., in NaCl 0.15 M; Sigma–Aldrich, USA) and placed in a stereotaxic frame for the implant of electrodes with body temperature maintained at 37 ± 0.5 °C by using a heating pad (Insight, Brazil). The level of anesthesia was maintained stable by supplementary doses of anesthetic (10% of the initial dose) and constantly checked by the tail pinch reflex, respiratory rate and EEG. In brief, the skull was exposed and small holes were drilled (all ipsilateral) to allow access to the lateral ventricle (antero-posterior, AP: −0.5 mm, lateral to midline, L: −1.3 mm, ventral to dura-mater, V: −2.53 mm); mPFC (AP: +3.0 mm, L: −0.5 mm, V: −3.1 to −3.4 mm) and dorsal-posterior region of CA1 (AP: −5.7 mm, L: −4.6 mm, V: −2.0 to −2.5 mm), according to Paxinos and Watson (2007). An additional contralateral hole was drilled to implant a recording ground micro-screw over the parietal cortex and all signals were referenced to it. A stainless-steel guide cannula (23 gauge), directed to the lateral ventricle, was inserted through a burr hole made on the skull and fixed into the bone with dental acrylic resin. The tip of the cannula was positioned 1 mm above the target injection site.

Teflon-insulated tungsten wires (60 μm diameter) were used to prepare stimulating and recording electrodes. A twisted bipolar electrode (vertical tip separation 500 μm) was used for constant current stimulation of CA1 and a single monopolar electrode was used to record field post-synaptic potentials (fPSP) in the prelimbic region of the mPFC. Both electrodes were lowered into the brain through holes made on the skull after removing the dura-mater. Their final positions were adjusted to obtain the highest negative-going response in the mPFC with latency to the first negative peak of 15–17 ms and amplitude ≥250 μV (Jay et al., 1995; Laroche et al., 1990; Lopes Aguiar et al., 2008). Monophasic test pulses (200 μs duration) were delivered every 20 s at increasing intensities (60–500 μA) and the resulting fPSPs were used to calculate input–output curves for each animal (S88 stimulator; Grass Instruments Co.). Based on these curves, we calculated the minimum intensity necessary to produce maximum mPFC fPSP responses and used 70% of this intensity to stimulate CA1 during baseline, low-frequency stimulation (LFS) and post-LFS recordings. Baseline fPSPs were recorded for 30 min before LFS induction with single test pulses of 200 μs duration, every 20 s. After LFS, fPSP recordings continued for 240 min to evaluate the dynamics of mPFC responses. LFS protocols used were: LFS600 (a sub-threshold protocol, induced by 600 trains of low frequency pulses) reported to promote a transient form of synaptic depression in the mPFC; and LFS900 (a supra-threshold protocol, induced by 900 trains of low frequency pulses) capable of producing a stable long-term depression (Takita et al., 1999). In both protocols, each train consisted of five pulses of 200 μs duration at 250 Hz, delivered every second. fPSPs were recorded after amplification and band-pass filtering (gain = 100×, 0.03–3 kHz; P55-AC pre-amplifier, Grass Instruments Co.), and subsequently digitized at 10 kHz (PowerLab/16S; Scope-AD Instruments). In order to test the muscarinic and NMDA modulation of cortical plasticity, we implanted a chemitrode (an electrode-cannula unit) into the mPFC for simultaneous drug injection and electrophysiological recording. Microinjections were carried out with a 30-gauge needle connected to a 10 μL-microsyringe (Hamilton Company, Reno, Nevada, USA) via polyethylene tubing. The needle was inserted into a 23-gauge guide cannula to deliver 1 μL (for i.c.v. injection) or 0.4 μL (for injection intra-mPFC) of drug over a period of two minutes. In order to control for spontaneous desynchronization before PILO, we monitored LFPs during this time and carried out the microinjections only when LFPs had predominantly delta waves for at least 2 min.

2.3. Long-term depression experiments

In order to study the pharmacological modulation of synaptic depression in the CA1–mPFC pathway, four experiments were carried out. Experiment I – tested the effects of pre-administration of PILO on transient depression induced by LFS600. Animals received an intracerebroventricular (i.c.v.) microinjection of PILO (40 nmol/μL in artificial cerebrospinal fluid, aCSF, 1 μL i.c.v., group: PILO + LFS600) or Veh (aCSF; group: Veh + LFS600) just before LFS600. aCSF had the following composition (in mM): 2.7 KCl, 1.2 $CaCl_2$, 1 $MgCl_2$, and 135 NaCl, pH 7.3, at room temperature (25 ± 0.5 °C). In addition, control groups assessed the effects of aCSF and PILO on basal mPFC fPSPs without LFS. Animals received a microinjection of PILO (40 nmol/μL in aCSF, 1 μL, i.c.v., group: PILO) or Veh (aCSF; group: Veh) after 30 min of baseline recordings, and fPSPs were monitored for additional 240 min. Experiment II: tested the effects of PILO administration following LFS600. Animals received a microinjection of PILO (40 nmol/μL in aCSF, 1 μL, i.c.v., group: LFS600 + PILO) or Veh (aCSF; group: LFS600 + Veh) 20 min after LFS600. Experiment III: tested the involvement of NMDA receptors in the muscarinic modulation of prefrontal depression. Animals received a microinjection of the competitive NMDA receptor antagonist, AP7 (10 nmol/μL in NaCl 0.15 M; 0.4 μL intra-mPFC; group: AP7 + PILO + LFS600) or Veh (NaCl 0.15 M; group: Veh + PILO + LFS600) 10 min before PILO (40 nmol/μL in aCSF, 1 μL, i.c.v.) and then received LFS600. Experiment IV: tested the effect of NMDA receptor inactivation on the LTD induced by LFS900. Animals received a microinjection of AP7 (10 nmol/μL in NaCl 0.15 M, 0.4 μL, intra-mPFC, group: AP7 + LFS900) or Veh (NaCl 0.15 M, group: Veh + LFS900) 10 min before LFS900 protocol. LTD was calculated as percentage of baseline levels measured during the first 30 min of baseline for each group. In each experiment, synaptic depression was evaluated by comparing 10-min averaged fPSPs (amplitude and slope values) during baseline and following LFS. Baseline recordings were identified as BL1: 0–10 min; BL2: 10–20 min and BL3: 20–30 min.

2.4. Local field potential recordings and analysis

Local field potentials (LFPs) were recorded in CA1 and mPFC through the same electrodes used to induce and record LTD, in order to monitor oscillatory brain activity during drug injections. In a pilot study, we defined the dose of PILO necessary to disrupt LFP delta oscillations in the hippocampus and mPFC long enough to last the LFS protocol (~15 min; Fig. 1A). In all the experiments, hippocampal and cortical LFPs were recorded for 6 min divided into 3 blocks of 2 min: before, during and after i.c.v. microinjections. For analysis, LFPs were initially down sampled (decimation to 500 Hz) and low-pass filtered (0.5–100 Hz). Welch's power spectral densities were estimated for epochs of 10 s, using a 625 s-points Hanning window, after averaging periodograms calculated from eight sections with 50% overlap. In addition, normalized power spectra in delta (0.5–4 Hz), theta (4–12 Hz), beta (12–30 Hz), gamma (30–80 Hz) as well as 25–45 Hz and 80–100 Hz bands were calculated using custom-made Matlab scripts (The MathWorks, Natick, MA). Signal power at 58–62 Hz was excluded from the spectra due to 60 Hz-noise contamination. Integrated power spectra at these bands were compared to evaluate the effect of PILO on CA1 and mPFC oscillatory activity. For time-frequency power spectrum calculation and coherence analysis, we used the *mtspscgramc*, *cohgramc* and *coherencyc* scripts from Chronux package, which calculate the moving window power spectrum, the averaged time-frequency multi-taper coherence and averaged coherence between two continuous signals (mPFC and CA1) with jackknife estimated 95% confidence interval, respectively (Bokil et al., 2010). Chronux parameters used: (movingwin = [6 1], fpass = [0 100], tapers = [3 5], err = [2 0.05], trialave = 1, pad = 0). To compare coherence values at different frequency bands of Veh and PILO groups we used Student's paired *t*-test on *z*-transformed coherences.

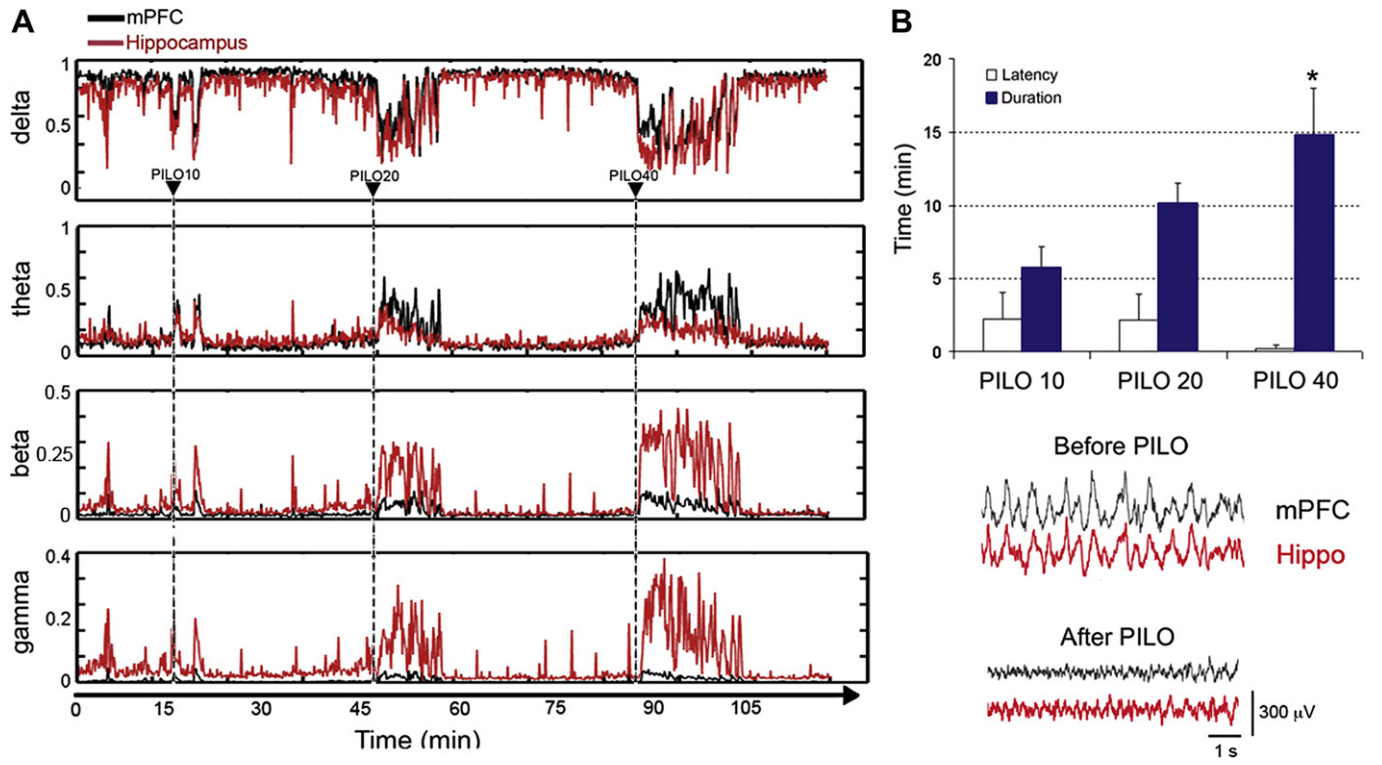

Fig. 1. Concentration-dependent effect of PILO on hippocampus and mPFC oscillatory activity during urethane anesthesia. A, Integrated power spectrum analysis at delta (0.5–4 Hz), theta (4–12 Hz), beta (12–30 Hz) and gamma (30–80 Hz) bands of a representative animal before and after drug administration (10, 20 and 40 nmol/μL; 1 μL; i.c.v.). LFPs were continuously recorded in the hippocampus and mPFC following microinjections of PILO at different concentrations for a total time of 2 h. Note that PILO suppressed slow waves and enhanced fast oscillations. B, *Above*, latency and duration of PILO effect ($n = 5$). *Below*, representative LFP tracings before and after PILO injection. Data are shown as mean ± S.E.M. Statistical difference was determined by one-way ANOVA followed by Bonferroni post-hoc test. $^{*}p < 0.05$, *vs.* PILO10 and PILO20.

In order to evaluate the relationship between the level of synchronization induced by PILO and the magnitude of mPFC synaptic depression, we calculated correlation coefficients between LFP power spectra at individual frequency bands following Veh or PILO injection and the averaged amplitude of cortical fPSPs 0–30 min and 30–60 min after LFS600. We used 128-s LFP epochs recorded in the CA1 and mPFC from 27 animals belonging to Veh–LFS ($n = 7$), PILO–LFS ($n = 7$), Veh–PILO–LFS ($n = 6$) and AP7–PILO–LFS ($n = 7$) groups. Correlation coefficients and 95% prediction intervals were calculated with home-written Matlab routines.

2.5. Histology for electrode positioning determination

After the experimental procedures, all animals received a brief current pulse (1 mA/1 s) through the stimulating and recording electrodes to mark tip placement by electrolytic lesion. Then, they received an additional dose of urethane (1.5 g/kg, i.p. in NaCl 0.15 M) and were decapitated. Their brains were removed, post-fixed in 10% formaldehyde-saline solution for 14 h at 4 °C and cryoprotected for 48 h in 20% sucrose solution (sucrose in 0.1 M sodium phosphate buffer pH 7.4). After freezing in dry ice-chilled isopentane, the brains were cut in 30 μm slices, mounted on gelatinized slides and processed for cresil violet staining. Electrode tip positions and cannula tracts were determined after analysis of the slides under a microscope using bright field (BX-60 Olympus, USA).

2.6. Statistical analysis

Two parameters of mPFC evoked responses (fPSPs) were analyzed: the amplitude of the negative deflection with latency at 15–17 ms, measured from the baseline after the stimulus artifact to the negative peak; and the slope of the fPSP, measured as the slope between two points in the descending curve of the fPSP – one at 1/4 and the other at 3/4 of its length. We used Student's *t*-test to compare baseline fPSP parameters between pairs of groups in each experiment. Analysis of group differences following LFS was carried out using a mixed model two-way ANOVA for repeated measures (group: fixed factor *vs.* time: repeated measures). Baseline fPSP data and power spectrum differences in the mPFC and CA1 were analyzed using one-way ANOVA for repeated measures and Student's *t*-test. For coherence analysis, we tested using two-way ANOVA for repeated measures and Student's paired *t*-test followed by Bonferroni correction. Bonferroni post-hoc tests were used following ANOVAs when necessary. Pearson's correlation coefficient followed by Student's *t*-test was used to test the correlation significance. Data are expressed as mean ± SEM (standard error of the mean) and significance level was set to 0.05.

3. Results

All animals included in our analysis had stimulating electrodes positioned in the dorsal aspect of the posterior CA1 area and recording electrodes positioned in the medial wall of the prefrontal cortex, corresponding to the prelimbic area of the mPFC. Metal cannulae were positioned 1 mm above the lateral ventricle with the microinjection needle reaching the target area. Reliable field evoked responses in the mPFC were obtained after CA1 stimulation and consisted of a negative deflection with average latency of 15.73 ± 0.2 ms, amplitude of 320 ± 10 μV and slope of −56.47 ± 2.5 μV/ms, as previously reported (Laroche et al., 1990; Lopes Aguiar et al., 2008; Romcy-Pereira and Pavlides, 2004). Table 1 shows the parameters of baseline cortical fPSPs measured for all experimental groups. No significant differences were detected in

Table 1
Descriptive statistics of mPFC evoked responses (fPSPs) obtained during baseline recordings in the absence of any drug. No statistical differences were observed among paired groups. Student's *t*-test was used to test statistical significance and data are shown as mean ± S.E.M.

Groups	Amplitude (mV)	Slope (μV/ms)	Latency (ms)
PILO + LFS600	0.33 ± 0.03	−57.19 ± 4.80	15.86 ± 0.44
Veh + LFS600	0.37 ± 0.04	−64.75 ± 5.23	16.14 ± 0.32
Veh	0.29 ± 0.03	−53.90 ± 5.39	15.63 ± 0.52
PILO	0.38 ± 0.03	−65.65 ± 7.02	15.50 ± 0.34
LFS + PILO	0.32 ± 0.01	−61.87 ± 2.66	15.13 ± 0.23
LFS + Veh	0.36 ± 0.04	−65.77 ± 6.33	14.99 ± 0.38
AP7 + PILO + LFS600	0.26 ± 0.02	−42.73 ± 3.70	16.54 ± 0.46
Veh + PILO + LFS600	0.28 ± 0.03	−47.93 ± 7.30	17.05 ± 0.22
AP7 + LFS900	0.29 ± 0.02	−56.01 ± 4.36	15.17 ± 0.40
Veh + LFS900	0.27 ± 0.03	−48.91 ± 6.02	15.27 ± 0.37

the average latency, amplitude or slope of the fPSPs between groups (Student's *t*-test, $p > 0.05$).

In a pilot study with 5 animals, CA1 and mPFC oscillatory activities were monitored continuously during 120 min in order to determine the latency and duration of the cholinergic theta synchronization after i.c.v. microinjection of different concentrations of PILO (10, 20 and 40 nmol/μL). Fig. 1A and B shows the concentration-dependent effect of PILO on hippocampus and mPFC oscillations. At higher concentrations, PILO dampened the urethane-associated delta more efficiently, as seen by the reduction in the latency to block the urethane-associated delta state (Fig. 1B) and concomitant increase in the duration of the delta power suppression. The decrease in delta was associated to an increase in theta, beta and gamma oscillations observed in CA1 and mPFC. In the hippocampus, beta and gamma oscillations showed an apparent higher increase as compared to the mPFC (Fig. 1A). This pattern of oscillatory changes was observed in all groups that received PILO (Fig. 2). At the highest concentration studied, 40 nmol/μL, PILO significantly shifted the LFP power balance from a state of predominant urethane-driven delta oscillations (0.5–4 Hz) to a state enriched in higher-frequencies (>4-Hz), for a period of time long enough to match the duration of the LFS protocol used to induce LTD (~15 min; Fig. 1B). Therefore, we chose this concentration of PILO to be used in our experiments. In addition, to certify that spontaneous desynchronized states initiated before PILO injection did not interfere with the interpretation of our data, we compared the power spectra at different bands of all groups before PILO. Our results did not show any difference between the groups (data not shown: mean of relative delta, theta, beta and gamma power for mPFC and Hippo; one-way ANOVA, $p > 0.05$).

Fig. 2 shows the power spectrum analysis of LFPs recorded from Veh- and PILO-treated animals. As we can see, both groups had similar power spectra in CA1 and mPFC prior to PILO administration (two-way ANOVA, $p > 0.05$, Fig. 2A1–B1). Following PILO, we readily observed that both areas underwent a global upward shift in their power spectra counteracting the slow wave state induced by urethane (two-way ANOVA, $p < 0.05$, Fig. 2A1–B1). We quantified the changes in four frequency bands and observed a clear suppression of delta (mPFC: $t(28) = 2.92$, $p < 0.05$; CA1: $t(28) = 3.48$, $p < 0.05$) and increase in theta (mPFC: $t(28) = 2.30$, $p < 0.05$; CA1: $t(28) = 3.62$, $p < 0.05$), beta (mPFC: $t(28) = 2.87$, $p < 0.05$; CA1: $t(28) = 1.89$, $p > 0.05$) and gamma (mPFC: $t(28) = 2.35$, $p < 0.05$; CA1: $t(28) = 3.06$, $p < 0.05$) oscillations following the muscarinic activation (Fig. 2A1–A3 and Fig. 2B1–B3).

In order to measure the effect of PILO on the oscillatory coupling between CA1 and mPFC, we also calculated the coherence of LFP epochs recorded before and after microinjection. Significant group effect (Veh *vs.* PILO) was detected only for coherences in the 25–45 Hz band ($F(1,28) = 4.92$, $p < 0.05$; two-way ANOVA) and 80–100 Hz band ($F(1,28) = 5.47$, $p < 0.05$). Paired *t*-test followed by Bonferroni correction showed that after PILO administration there was a significant decrease in hippocampo-cortical coherence in delta (0.5–4 Hz; $t(19) = 3.70$, $p < 0.01$) and 80–100 Hz band ($t(19) = 3.07$, $p < 0.01$), as well as an increase in coherence in the 25–45 Hz band ($t(19) = 3.28$, $p < 0.01$; Fig. 3). In Veh-treated animals, we did not detect any significant change in coherence (Student's paired *t*-test, $p > 0.05$).

3.1. Muscarinic receptor activation converts sub-threshold transient depression induced by LFS600 into a long-lasting LTD in the mPFC in vivo

We tested the effect of brain muscarinic activation on the transient depression of mPFC responses induced by sub-threshold CA1 stimulation by applying PILO (40 nmol; i.c.v.) before LFS600 and monitoring prefrontal fPSPs for 4 h. Fig. 4 shows that PILO converted the transient depression induced by LFS600 stimulation into a robust long-lasting LTD with average duration of 4 h. PILO produced an average decrease of 18% in mPFC fPSP amplitude over the entire recording session (4 h) (PILO + LFS600 *vs.* Veh + LFS600: fPSP amplitude, $F(1,23) = 8.64$, $p < 0.05$); fPSP slope, $F(1,23) = 5.53$, $p < 0.05$; two-way ANOVA for repeated measures, Fig. 4A–D). Both the induction (+12–14%; PILO + LFS600 *vs.* Veh + LFS600; fPSP amplitude: first 30 min post-LFS600, $p < 0.05$; fPSP slope: first 30 min post-LFS600, $p < 0.05$; Student's *t*-test) and the maintenance of synaptic depression were potentiated by pre-LFS muscarinic activation as compared to Veh-injected control group (+18 to +27%; PILO + LFS600 *vs.* Veh + LFS600; fPSP amplitude: 60–210 min post-LFS600, $p < 0.05$; fPSP slope: 70–150 min post-LFS600, $p < 0.05$; ANOVA followed by Bonferroni post-hoc test, Fig. 4A and B). Fig. 5 shows that PILO by itself did not change the magnitude of basal synaptic transmission in the CA1-mPFC pathway as compared to control (PILO *vs.* Veh: fPSP amplitude, $F(1,23) = 0.03$, $p > 0.05$; fPSP slope, $F(1,23) = 0.02$, $p > 0.05$; two-way ANOVA for repeated measures).

3.2. Post-LFS600 muscarinic receptor activation has little effect on sub-threshold transient depression in mPFC

In order to evaluate the time-dependence effect of PILO on the enhancement of mPFC synaptic depression, we microinjected PILO 20 min after CA1 LFS600 stimulation. Our results show that post-LFS PILO administration does not change the amplitude of prefrontal responses following LFS600, as compared to the control group. There was no statistically significant effect on fPSP amplitude or fPSP slope between LFS600 + PILO and LFS600 + Veh groups (Fig. 6A–D); LFS600 + PILO *vs.* LFS600 + Veh: fPSP amplitude, $F(1,23) = 2.35$, $p > 0.05$); fPSP slope, $F(1,23) = 2.04$, $p > 0.05$; two-way ANOVA for repeated measures). Both the induction and the maintenance of the synaptic depression were unaffected by post-LFS muscarinic activation (see also Fig. 7).

3.3. NMDAR blockade impairs the muscarinic facilitation of mPFC synaptic depression

In order to investigate the involvement of NMDA-dependent mechanisms on the muscarinic modulation of mPFC synaptic depression, we applied AP7 (10 nmol/μL; 0.4 μL) directly into the mPFC of rats, 10 min before the injection of PILO or Veh. Fig. 8 shows that blocking NMDAR in the mPFC altered the modulatory effect of PILO on prefrontal synaptic plasticity. AP7 prevented PILO from converting the transient depression induced by LFS600 into long-lasting LTD (−13%, AP7 + PILO + LFS600 *vs.* Veh + PILO + LFS600: fPSP amplitude, $F(1,23) = 4.83$, $p < 0.05$); fPSP slope, $F(1,23) = 6.46$, $p < 0.05$; two-way ANOVA for repeated measures, Fig. 8C and D). AP7 attenuated LTD induction and impaired the late-phase enhancement of transient depression (−16 to −22%; AP7 + PILO + LFS600 *vs.* Veh + PILO + LFS600; fPSP amplitude: 170–240 min post-LFS600, $p < 0.05$; fPSP slope: 130–240 min post-LFS600, $p < 0.05$; Fig. 8C).

Although PILO had a conspicuous overall effect of reducing delta and promoting >4-Hz oscillations in Veh- and AP7-treated rats (Fig. 8A and B), the prior application of AP7 seems to have particularly attenuated the >4-Hz-promoting effect of PILO in the mPFC as compared to the hippocampus (Fig. 8B). AP7 also reduced PILO-induced power peaks at ~5 Hz in the mPFC ($p < 0.05$, Student's *t*-test) and ~9 Hz in CA1 ($p < 0.05$, Student's *t*-test; Fig. 8B, *inset*), suggesting that oscillatory changes due to intra-mPFC AP7 were not restricted to the mPFC as expected.

Moreover, the sole effect of AP7 in the absence of PILO, i.e. before PILO injection, showed that blocking NMDAR in the mPFC induces

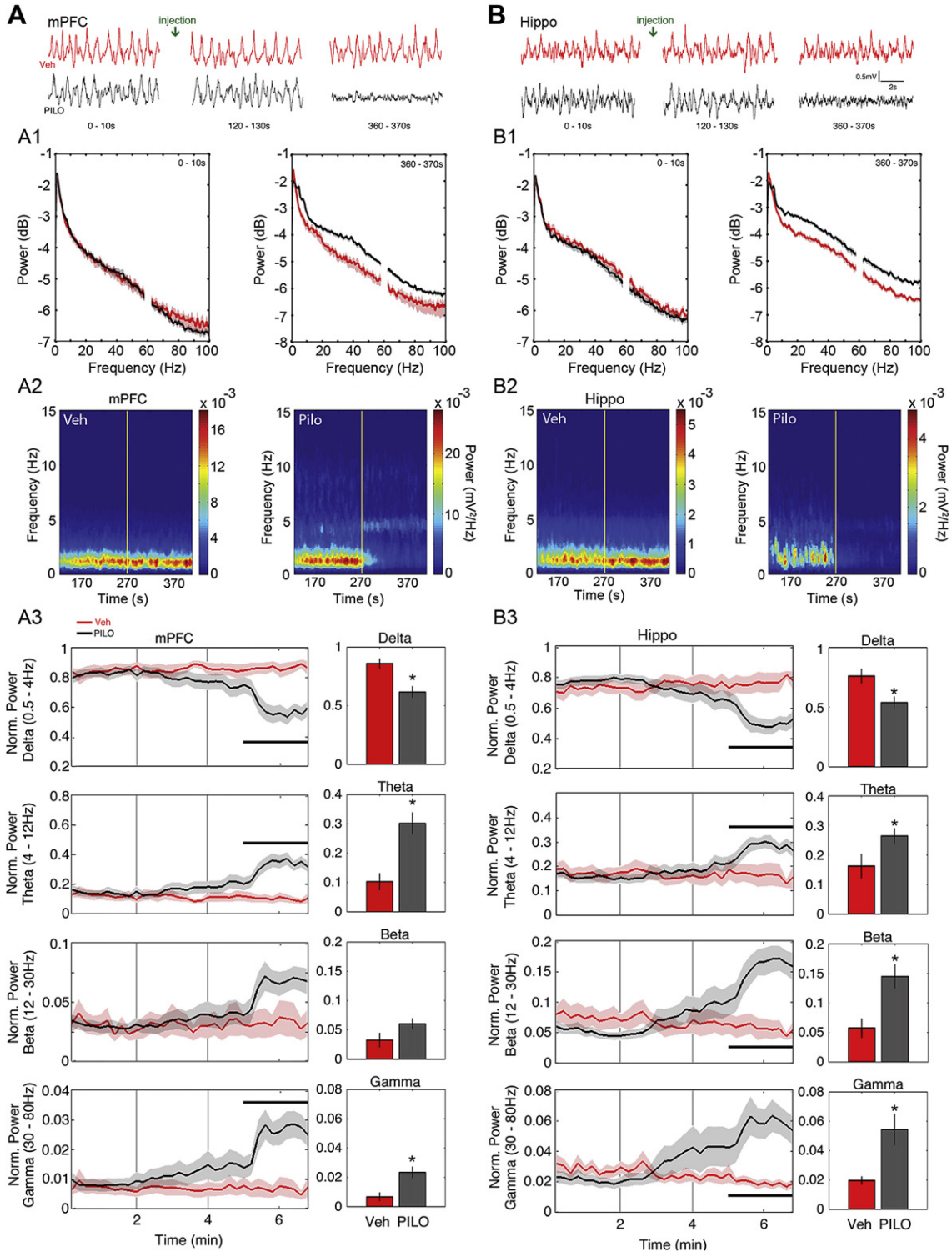

Fig. 2. Power spectrum analysis of LFPs recorded during the experiments. LFPs in the mPFC (A) and hippocampus (B) following injection of PILO (40 nmol/μL; 1 μL, i.c.v.) and Veh (aCSF; 1 μL, i.c.v.). *Above*, Representative tracings recorded before (0–10 s), during (120–130 s) and after (360–370 s) drug injection. Group averaged power spectra calculated from 10 s-epochs recorded before and after PILO administration (A1–B1) and averaged time-frequency spectra around injection time (A2–B2; *yellow vertical line* represents the end of drug microinjection) shows the effects of PILO. A3–B3, Relative power spectra calculated for Veh and PILO animals. Significant differences between groups are indicated by the horizontal black bar in each graph and illustrated in the bar graph on the left (Veh, $n = 10$; PILO, $n = 20$). Vertical lines define time windows before, during and after PILO microinjection. Noise power (58–62 Hz) was removed from plots. Data are shown as mean ± S.E.M. Differences were tested using Student's *t*-test, $^{*}p < 0.05$, *vs.* Veh group.

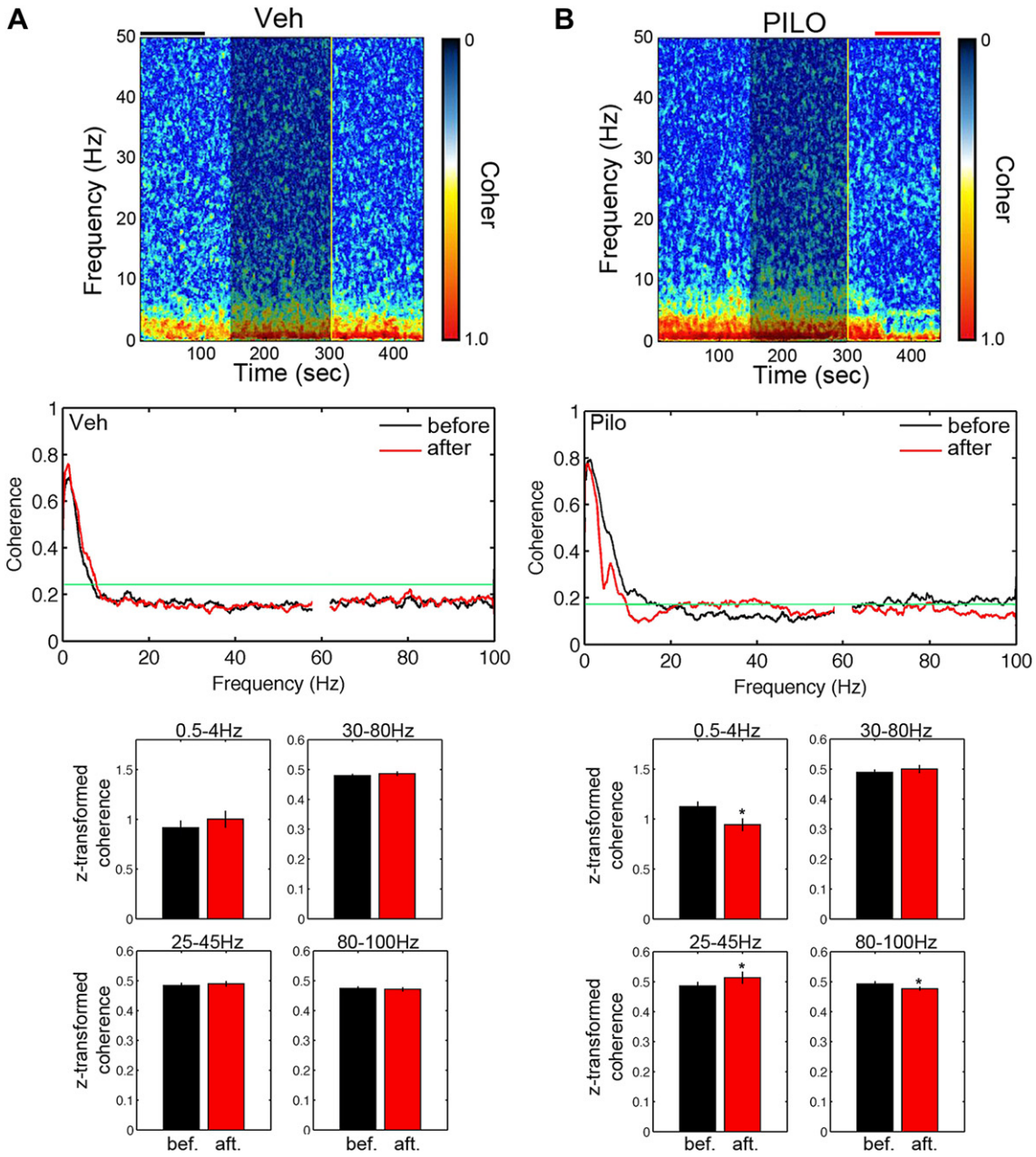

Fig. 3. Spectral coherence between the mPFC and the hippocampus following Veh and PILO microinjections (Veh, $n = 10$; PILO, $n = 20$). A–B (*above*), Averaged coherograms illustrate changes in mPFC-Hippo coherence after Veh and PILO microinjections, respectively. *Shaded area* represents time during drug injection. Color-coded coherence values represent values above threshold determined by a jack-knife 95% confidence interval. *Middle*, Coherence calculated in a 128 s-window before (0–128 s; *black bar in the coherogram*) and after (336–464 s; *red bar in the coherogram*) the microinjections. *Green line* depicts 95% confidence interval. *Below* (*bar graph*), In animals that received PILO, we observed a significant increase in the 25–45 Hz band coherence ($p < 0.05$), and a decrease in delta (0.5–4 Hz; $p < 0.05$) and 80–100 Hz band coherences ($p < 0.05$) as we compared coherences before and after drug injection. In controls, no significant differences were observed after Veh administration. Data are shown as mean ± S.E.M. Differences were tested using Student's paired *t*-test followed by Bonferroni correction, $^{*}p < 0.05$, *before vs. after injection*.

an increase in delta (mPFC: $F(1,137) = 56.16$, $p < 0.05$; CA1: $F(1,137) = 28.81$, $p < 0.05$) and a reduction in oscillations >4-Hz ($p < 0.05$, two-way ANOVA; Fig. 8B) both in CA1 and mPFC as compared to control animals (Fig. 8B).

3.4. NMDAR antagonism impairs LTD induced by LFS900 in the mPFC

In the mPFC, long-lasting LTD can be induced by applying 900 pulses of LFS in the hippocampus in the absence of PILO. Here, we decided to test whether the same concentration of AP7 used to block the long-lasting LTD induced by sub-threshold stimulation in the presence of PILO could also impair LTD induced by LFS900. In this experiment, we applied AP7 directly into the mPFC (10 nmol/μL; 0.4 μL) 10 min before LFS900 stimuli. Fig. 9 shows that AP7 applied into the mPFC strongly impairs the expression of LFS900-induced cortical LTD (−13%, AP7 + LFS900 *vs.* Veh + LFS900: fPSP amplitude, $F(1,23) = 7.06$, $p < 0.05$); fPSP slope, $F(1,23) = 7.09$, $p < 0.05$; two-way ANOVA for repeated measures, Fig. 9D). Post-hoc analysis showed that AP7 blocked both the induction and the maintenance of the LFS900-induced LTD in the mPFC *in vivo* (−18 to −25%; AP7 + LFS900 *vs.* Veh + LFS900; fPSP amplitude:

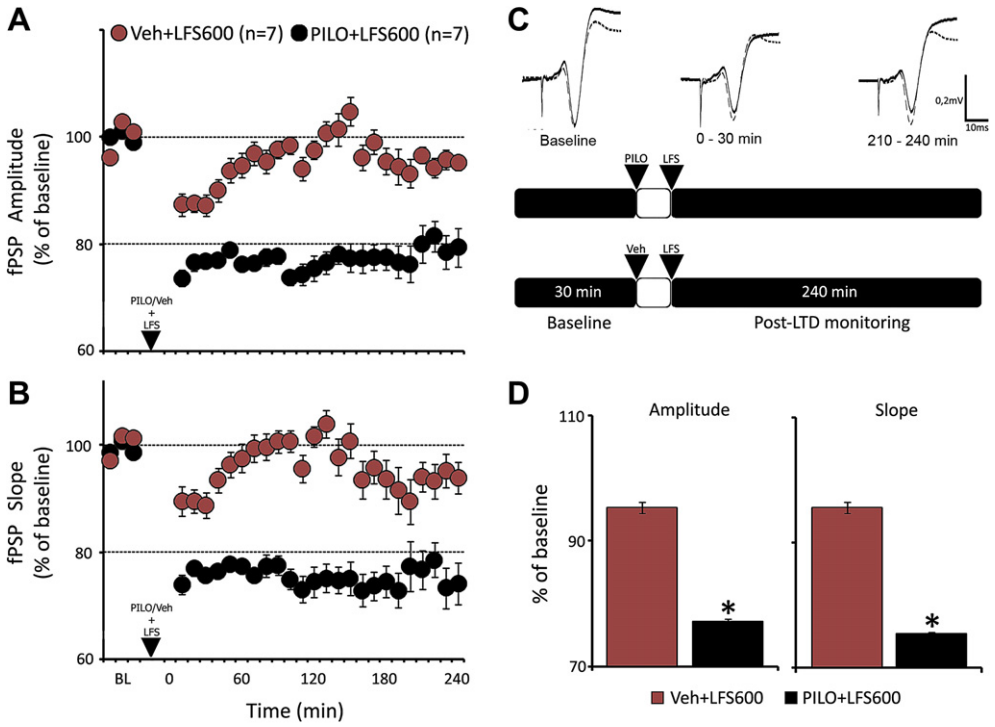

Fig. 4. Muscarinic pre-activation enhances the effects of sub-threshold LFS (LFS600) inducing a long-lasting cortical LTD. A–B, Microinjection of PILO immediately before LFS600 enhances the transient depression of synaptic responses in the mPFC as measured by the fPSP amplitude and slope. C, Experimental design showing representative fPSPs recorded in the mPFC during baseline (30 min) and monitored for additional 240 min after sub-threshold LFS. PILO (40 nmol; i.c.v.) or Veh (aCSF) were microinjected just before LFS600 protocol. Representative fPSPs are shown aligned to the time scale of the experimental paradigm (black line: PILO + LFS600 group; dashed line: Veh + LFS600 control group). D, Averaged effect of PILO on mPFC fPSPs following LFS. PILO pre-treatment significantly enhances synaptic depression promoting an overall LTD effect when compared to control group. Data are shown as mean ± S.E.M. Group differences were calculated by two-way ANOVA with repeated measures followed by Bonferroni post-hoc test: $^{*}p < 0.05$ *vs.* control group.

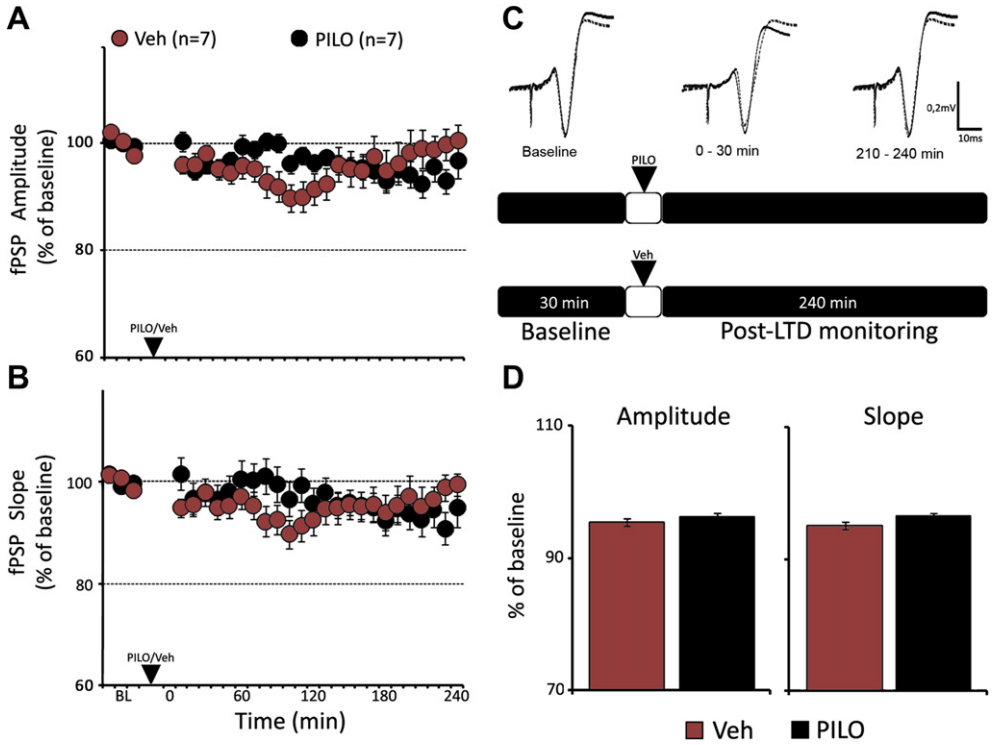

Fig. 5. PILO does not affect basal synaptic transmission in the mPFC. A–B, PILO microinjection did not affect basal fPSPs recorded in the mPFC when measure by the amplitude and slope of fPSPs. C, Experimental design showing representative fPSPs recorded in the mPFC during baseline (30 min) and monitored for additional 240 min after PILO (40 nmol/μL; i.c.v.) or Veh (aCSF) microinjection. Representative fPSPs are shown aligned to the time scale of the experimental paradigm (black line: PILO group; dashed line: Veh control group). D, Averaged effect of PILO on basal mPFC fPSPs. PILO did not change significantly the magnitude of cortical fPSPs. Data are shown as mean ± S.E.M. Statistical analyses were calculated by two-way ANOVA with repeated measures.

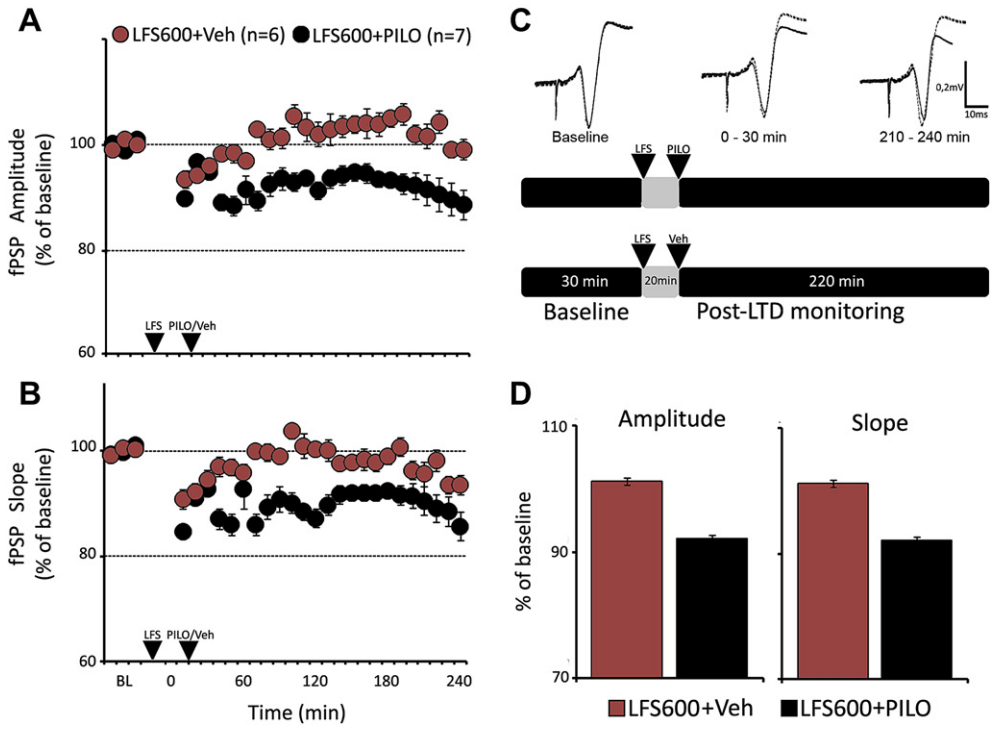

Fig. 6. Muscarinic post-activation does not affect significantly mPFC responses to sub-threshold LFS. A–B, Microinjection of PILO 20 min after LFS600 did not change cortical responses as measured by fPSP amplitude and slope. Although slightly reduced responses were observed, no group effect was detected using a two-way ANOVA with repeated measures. C, Experimental design showing representative fPSPs recorded in the mPFC during baseline (30 min) and monitored for additional 240 min after sub-threshold LFS. PILO (40 nmol/μL; i.c.v.) or Veh (aCSF) were microinjected 20 min after LFS600 protocol. Representative fPSPs are aligned to the time scale of the experimental paradigm (black line: LFS600 + PILO group; dashed line: LFS600 + Veh control group). D, Averaged effect of PILO following LFS600 as compared to control group. Data are shown as mean ± S.E.M.

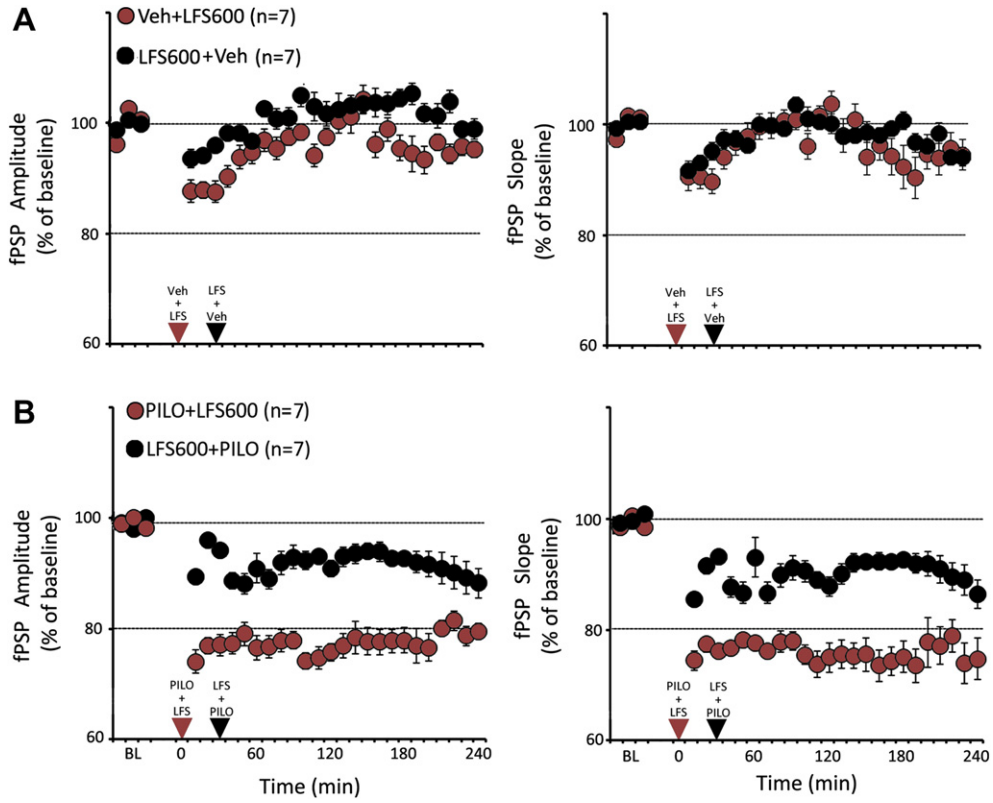

Fig. 7. A, Comparison of the effects of pre-LFS600 and post-LFS600 application of Veh (NaCl 0.15 M) on prefrontal cortex synaptic depression. B, Comparison of the effects of pre-LFS600 and post-LFS600 application of PILO (40 nmol/L) on prefrontal cortex evoked responses.

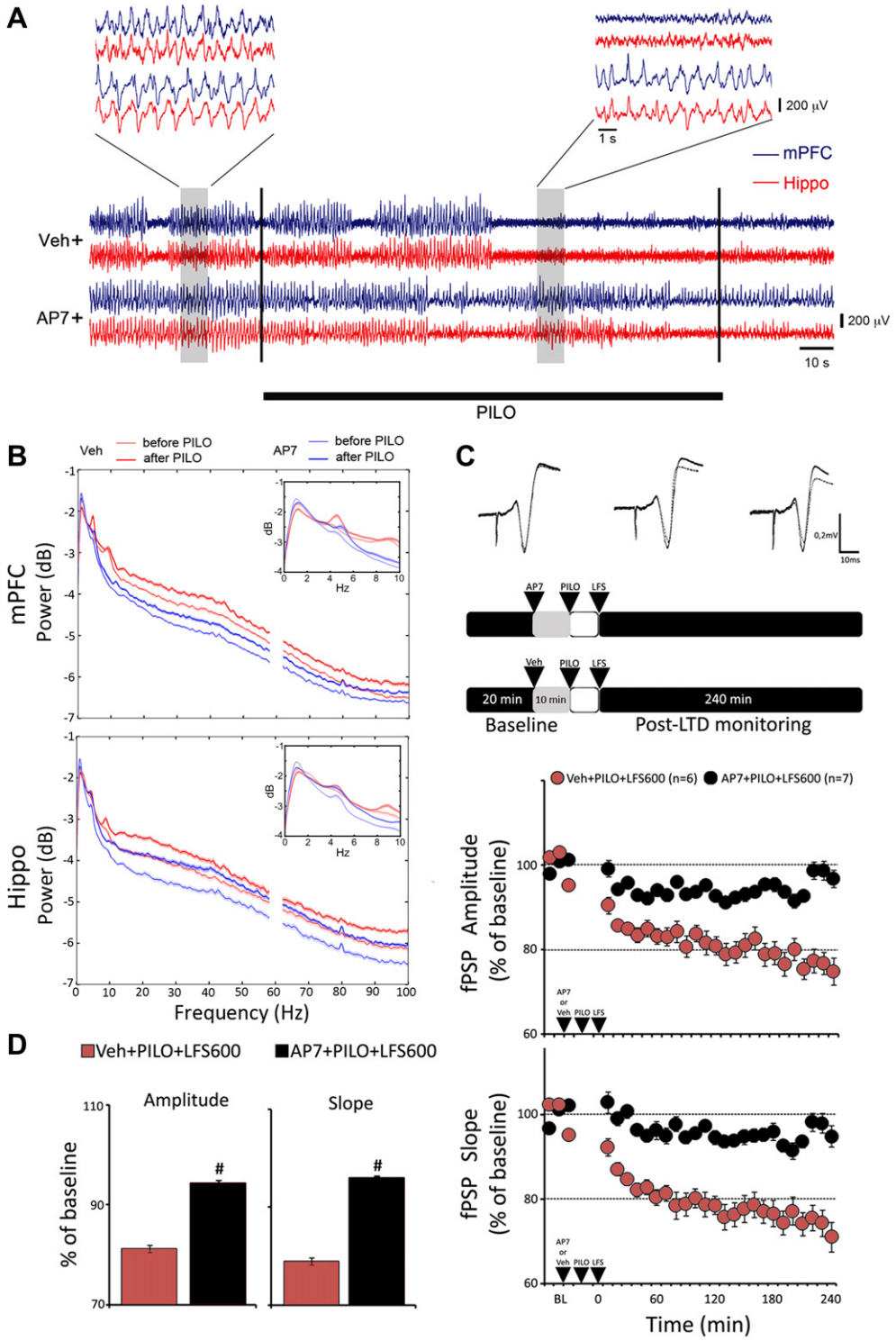

Fig. 8. NMDAR antagonist, AP7 prevents the enhancement of synaptic depression induced by PILO following sub-threshold LFS. A, Representative LFP tracings from the hippocampus and mPFC before and after drug microinjection in a Veh- and AP7-treated animal. Expanded LFPs are shown in the *insets*. Vertical black bars indicate onset and offset of PILO i.c.v. microinjection. B, Group averaged power spectra calculated from 10 s-epochs recorded in the mPFC and Hippo before and after PILO administration in Veh- and AP7-treated animals. PILO significantly decreased delta and increased >4 Hz oscillations in both Veh and AP7 groups (all frequency bands: ANOVA, $p < 0.05$). Preceding PILO injections, AP7 had the opposite effect on oscillations as compared to Veh controls. Noise power (58–62 Hz) was removed from plots. C, Experimental design showing fPSPs recorded in the mPFC during baseline (30 min) and monitored for additional 240 min after weak LTD induction. AP7 (10 nmol/μL; intra-mPFC) or Veh (NaCl 0.15 M) were applied 10 min prior to PILO (40 nmol/μL; i.c.v.). Representative fPSPs are aligned to the time line of the experimental paradigm (*solid line*: AP7 + PILO + LFS600 group; *dashed line*: Veh + PILO + LFS600 control group). *Below*, Time-course of cortical evoked responses. Intracortical application of AP7 prior to PILO i.c.v. microinjection prevented the long-lasting depression of synaptic responses induced by muscarinic pre-activation. D, Averaged effect of AP7 on mPFC synaptic responses following PILO + LFS600. Data are shown as mean ± S.E.M. Group differences were calculated by two-way ANOVA with repeated measures followed by Bonferroni post-hoc test: #$p < 0.05$ *vs.* control group.

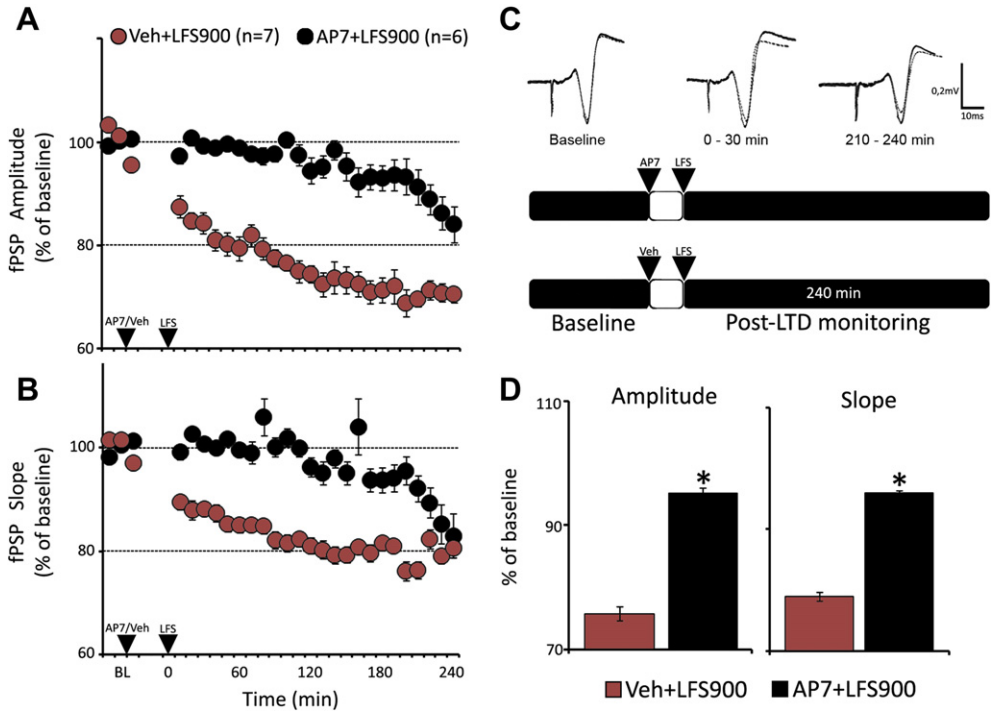

Fig. 9. AP7 blocks long-lasting LTD induced by a supra-threshold LFS (LFS900). A–B, Time-course of cortical evoked responses following intracortical microinjection of AP7. C, Experimental paradigm showing fPSPs recorded in the mPFC during baseline (30 min) and monitored for additional 240 min after supra-threshold LFS. AP7 (10 nmol/μL; 0.4 μL intra-mPFC) or Veh (NaCl 0.15 M) were applied 10 min before LFS900. Representative fPSPs are aligned to the time scale of the experimental paradigm (black line: AP7 + LFS900 group; dashed line: Veh + LFS900 control group). D, Averaged effect of AP7 treatment on mPFC LTD. Data are shown as mean ± S.E.M. Group differences were determined by two-way ANOVA with repeated measures followed by Bonferroni post-hoc test: $^{*}p < 0.05$ *vs.* control group.

40–210 min post-LFS600, $p < 0.05$; fPSP slope: 50–160 min post-LFS600, $p < 0.05$; Bonferroni post-hoc test, Fig. 9A and B). Although a delayed decay of mPFC responses have been observed in the last hour of recording, the post-hoc test showed no statistical differences in the AP7 + LFS900 intra-group analysis, indicating no LTD effect (comparisons: 10–240 min after LFS900 counter the baseline: BL1, BL2 and BL3; $p > 0.05$, Bonferroni).

3.5. Magnitude of gamma oscillation correlates to mPFC synaptic depression

In order to test whether the level of synchronization induced by PILO was correlated to the magnitude of LTD induction, we calculated linear correlation between LFP power spectra at different frequency bands following Veh or PILO injection and the amplitude of cortical fPSPs following a sub-threshold LTD stimulation protocol. All animals ($n = 27$) in the groups Veh-LFS600, PILO-LFS600, Veh-PILO-LFS600 and AP7-PILO-LFS600 were used. Our results show that gamma oscillations in the mPFC and hippocampus are significantly correlated to the amplitude of prefrontal fPSPs following LFS600 (mPFC: $r = -0.41$, $p = 0.03$; Hippo: $r = -0.55$, $p < 0.01$; Fig. 10). The higher the gamma power induced by drug microinjection, the lower the synaptic responses in the mPFC (i.e. higher levels of synaptic depression) following LFS. We also observed that theta power in the hippocampus, but not in the mPFC, was negatively correlated to the amplitude of cortical fPSPs ($r = -0.56$; $p < 0.01$). Delta and beta oscillations showed no correlation to cortical responses following LFS600 (Fig. 10).

4. Discussion

Numerous studies support the fact that cholinergic afferents to the frontal cortex mediate sustained attention, working memory and perceptual processing, which can be dysfunctional in many psychiatric disorders. Since the mPFC is a major cortical target of the hippocampal information outflow, studies on the synaptic modulation of CA1–mPFC circuitry may provide new insights about the mechanisms involved in cognitive, motivational and emotional impairments observed in these disorders. Here, we investigated in urethane-anesthetized rats, the modulatory effect of the muscarinic agonist PILO, on CA1–mPFC synaptic plasticity induced by sub- and supra-threshold low-frequency stimulation. We provide a first evidence of the muscarinic enhancement of synaptic depression in the mPFC following sub-threshold stimulation of CA1 inputs, the dependency of this effect on NMDA activation and the significant positive correlation between hippocampus and mPFC gamma power and prefrontal synaptic depression.

Our data show that PILO converts a transient cortical depression induced by sub-threshold LTD protocol (LFS600) into a robust LTD, stable for at least 4 h. Besides, we demonstrate that cortical NMDAR activation is involved in the muscarinic enhancement of mPFC synaptic depression, since AP7 microinjection into the mPFC blocked the conversion of transient depression into long-lasting LTD produced by PILO. Additionally, we observed that: (1) PILO does not affect mPFC responses when applied after LFS600; (2) LTD induced by supra-threshold protocol (LFS900) is also dependent on NMDAR activation; (3) PILO by itself does not alter basal synaptic transmission in the hippocampus–mPFC circuit; and (4) the muscarinic activation induced by PILO (40 nmol) produced a rapid and persistent displacement of slow-wave (0.5–4 Hz) by fast oscillations (5–80 Hz), which resulted in a significant negative correlation between the amplitude of prefrontal fPSPs after drug application and the hippocampal and mPFC gamma powers. Altogether, our findings suggest an important modulatory effect of the muscarinic neurotransmission on prefrontal-cortical synaptic plasticity and indicate the existence of a limited temporal window

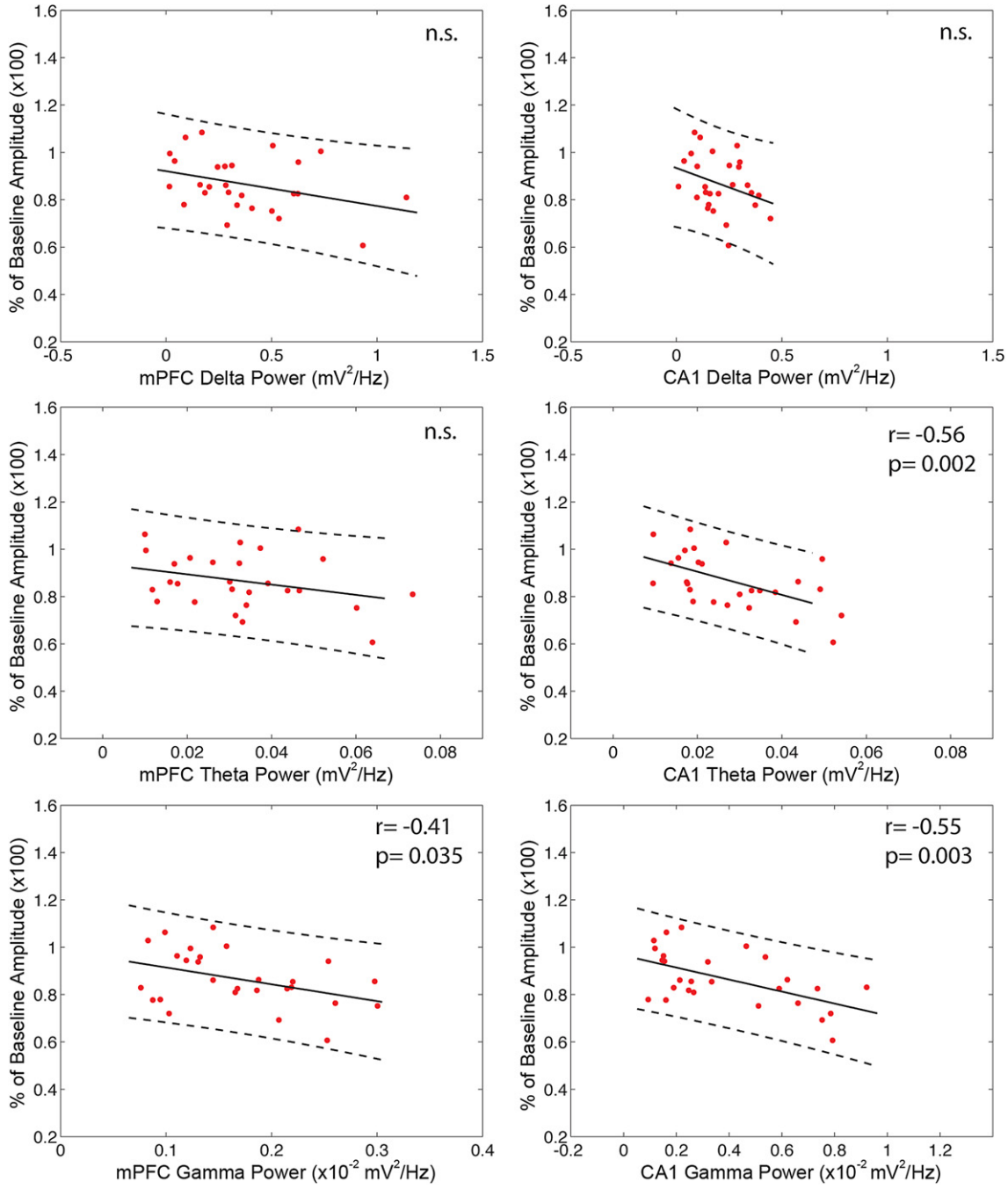

Fig. 10. The magnitude of theta and gamma oscillations negatively correlate with mPFC synaptic responses following LFS600. Linear correlation between integrated power spectrum at distinct frequency bands showed a significant negative correlation between averaged mPFC fPSPs 30 min after sub-threshold LFS and the hippocampus theta (4–12 Hz) and gamma (30–80 Hz) power, as well as the cortical gamma power. Dashed lines indicate 95% prediction interval.

for the effective modulation of PILO that requires NMDAR activation. Finally, the muscarinic conversion of transient cortical depression (induced by LFS600) into a robust LTD, shares similar NMDAR dependency with the LTD induced by supra-threshold protocol.

Prefrontal synaptic plasticity, expressed as LTP or LTD, can be induced or modulated by different neurotransmitter systems through a great diversity of receptors (Del Arco and Mora, 2009; Goto et al., 2010). In particular, the cholinergic system has an important role in cognitive processes mediated by the mPFC, though it has been less explored experimentally. In a previous report, we showed that PILO produced a significant enhancement of mPFC responses expressed 2 h after tetanic stimulation of CA1 *in vivo*. This was interpreted as a positive muscarinic effect on LTP maintenance instead of LTP induction, which could influence the information processing in the mPFC (Lopes Aguiar et al., 2008). Nonetheless, we showed here that PILO converted a sub-threshold transient depression induced by LFS600 into a long-lasting LTD. In fact, the robust synaptic depression induced by PILO followed by LFS600 contrasts with its enhancing effect on LTP following high-frequency stimulation. Such asymmetry in prefrontal responses to hippocampal HFS and LFS may represent an important modulatory switch for cortical synaptic plasticity during different brain

activation states. As a consequence, high CA1 firing rates under muscarinic activation would enhance the late-phase of LTP in the mPFC, whereas low firing rates under muscarinic activation would induce a robust and long-lasting depression of cortical synaptic responses. Although we cannot rule out indirect effects of PILO on brain circuits modulating prefrontal function (Gurden et al., 2000; Huang and Hsu, 2010; Kruse et al., 2009; Ohashi et al., 2003; Zhang et al., 2010), these results reveal the ability of the brain muscarinic system to exert a dual regulatory control of prefrontal synaptic plasticity (LTP or LTD) *in vivo*.

Theta rhythm is a characteristic oscillatory mode of the hippocampus modulated by septal cholinergic afferents through the activation of muscarinic receptors in the hippocampus (Buzsaki et al., 1983; Lee et al., 1994). Recent studies have shown that prefrontal cortical activity is coupled to the phase of the hippocampal theta oscillation in different behavioral tasks suggesting a hippocampal functional entrainment of cortical circuitries during particular demands (Brockmann et al., 2011; Hyman et al., 2005; Siapas et al., 2005). Considering the important role of the muscarinic modulation of hippocampal theta rhythm, it is plausible to think that in our experiments PILO could have modified the oscillatory coupling between the hippocampus and mPFC. Although, we did not record prefrontal spike activity, precluding the calculation of phase coupling, PILO induced a significant decrease in delta (0.5–4 Hz) and 80–100 Hz band coherences between CA1 and mPFC, and an increase in the coherence in the 25–45 Hz band. Our results also indicate a significant negative correlation between mPFC and hippocampal gamma power and the amplitude of prefrontal fPSPs following LFS600. This is consistent with previous reports showing that carbachol-induced theta and gamma oscillations in the hippocampus facilitate the conversion of LTP into LTD in CA1 *in vitro* (Huerta and Lisman, 1995). Kirkwood et al. (1999) also reported that carbachol facilitates LTD in the visual cortex by the activation of M1 muscarinic receptors, and Warburton et al. (2003) demonstrated that scopolamine impairs LTD induction, but has no effect on LTP in the perirhinal cortex.

It is known that hippocampal neurons in the postero-dorsal and ventral CA1/subiculum project direct axon terminals to the mPFC, where they establish excitatory synapses with dendritic spines of pyramidal neurons in layers II/III and V/VI (Groenewegen et al., 1997; Jay et al., 1992). These projections can undergo both LTP and LTD, though only LTP was shown to be dependent on NMDA receptor activation (Jay et al., 1995; Takita et al., 1999). Interestingly, our results show that both LTD induced by PILO/LFS600 and LTD induced by supra-threshold stimulation (LFS900) depend on prefrontal cortex NMDA receptor activation. In fact, they are consistent with reports showing that intracortical LTD in layer V of the mPFC induced by activation of group II metabotropic glutamate (mGluR) depends upon NMDA receptor activation (Huang and Hsu, 2008), M1/M3 muscarinic conversion of LTP into LTD in the dorsal cochlear nucleus requires functional NMDA receptors (Zhao and Tzounopoulos, 2011) and that acetylcholine, acting through M1 receptors, potentiates NMDA responses in the striatum (Calabresi et al., 1998). These studies support the idea of either a direct interaction between muscarinic and NMDA receptors in the expression of mPFC LTD or an indirect effect via the mesocortical dopaminergic system, known to modulate synaptic plasticity in the mPFC via cholinergic inputs. Previous reports have also shown that either noradrenaline acting through $\alpha1-\alpha2$ receptors or low levels of dopamine can induce NMDA-dependent LTD in the intrinsic connections of the mPFC (Marzo et al., 2010; Matsuda et al., 2006). Surprisingly, the supra-threshold LTD induced by strong electrical stimulation was also blocked by AP7, suggesting the activation of similar molecular mechanisms required to trigger the long-lasting LTD in the mPFC induced by PILO-LFS600.

Although AP7 apparently attenuated the synchronizing effects of PILO in the mPFC, the effects of NMDA blockade in the oscillatory brain activity following intra-mPFC microinjection, occurred both in the mPFC and the hippocampus. We also observed a significant reduction in ~5 Hz power in mPFC and ~9 Hz power in CA1 as compared to Veh-injected controls, which might suggest an indirect modulatory effect of the mPFC on areas projecting to the hippocampus, i.e., septum, thalamus or amygdala, as previously described (Lee et al., 1994; Seidenbecher et al., 2003).

PILO also exerted a more intense depressive effect on prefrontal post-synaptic responses when applied before LFS600, as opposed to after LFS600. The distinct effects of PILO on pre-LFS600 and post-LFS600 LTD suggest a limited temporal window of efficacy. Such priming could reflect the pre-activation of post-synaptic M1 receptors enhancing NMDA currents in mPFC neurons (Calabresi et al., 1998). In contrast to recent studies indicating an association between muscarinic activation and AMPA-receptor internalization during a muscarinic-induced LTD *in vitro* (Dickinson et al., 2009; Huang and Hsu, 2010; McCoy and McMahon, 2007), we showed that PILO by itself does not interfere with basal hippocampus–mPFC fPSPs *in vivo*.

The occurrence of bidirectional synaptic plasticity in the cortex is thought to be an important mechanism regulating the balance of cognitive and emotional processing. Dorsal and ventral hippocampal projections to the entorhinal cortex and mPFC undergo LTP, LTD and many forms of short-term synaptic changes, which are regularly modulated by the muscarinic cholinergic system (Laroche et al., 2000; Lopes Aguiar et al., 2008; Yun et al., 2000). Therefore, changes in the cholinergic drive on the hippocampal inputs to the mPFC are potential targets for neurological dysfunctions and have been implicated in cognitive and emotional deficits (Bymaster et al., 2002; Hasselmo, 2006; Leite et al., 1990, 2002; Lucas-Meunier et al., 2003; Raedler et al., 2007; Romcy-Pereira and Pavlides, 2004; Romcy-Pereira et al., 2009; Scarr and Dean, 2008).

In conclusion, the present study brings new evidence on the interaction of the muscarinic and NMDA modulation of synaptic depression in the mPFC, and the relationship between oscillatory gamma rhythm in limbic-cortical circuits and hippocampus–mPFC communication. It may contribute to our understanding of plasticity-related dysfunctions associated to cognitive and emotional deficits in psychiatric disorders.

Acknowledgments

We would like to thank Renata Scandiuzzi and Renato Meirelles for their excellent technical support, Matheus Rossignoli for valuable discussions and Dr. John McNamara for valuable comments on the paper. We also thank the two anonymous reviewers that helped to improve the paper. This work was supported by grants from FAPESP (#2007/57484-9 and #2009/54410-0), FAPESP-CInAPCe (#2005/56447-7) and CNPq (#502726/2009-1).

References

Bear, M.F., Kirkwood, A., 1993. Neocortical long-term potentiation. Curr. Opin. Neurobiol. 3, 197–202.
Bliss, T.V., Collingridge, G.L., 1993. A synaptic model of memory: long-term potentiation in the hippocampus. Nature 361, 31–39.
Bokil, H., Andrews, P., Kulkarni, J.E., Mehta, S., Mitra, P.P., 2010. Chronux: a platform for analyzing neural signals. J. Neurosci. Methods 192, 146–151.
Brockmann, M.D., Poschel, B., Cichon, N., Hanganu-Opatz, I.L., 2011. Coupled oscillations mediate directed interactions between prefrontal cortex and hippocampus of the neonatal rat. Neuron 71, 332–347.
Buonomano, D.V., Merzenich, M.M., 1998. Cortical plasticity: from synapses to maps. Annu. Rev. Neurosci. 21, 149–186.
Buzsaki, G., Leung, L.W., Vanderwolf, C.H., 1983. Cellular bases of hippocampal EEG in the behaving rat. Brain Res. 287, 139–171.

Bymaster, F.P., Felder, C., Ahmed, S., McKinzie, D., 2002. Muscarinic receptors as a target for drugs treating schizophrenia. Curr. Drug Targets CNS Neurol. Disord. 1, 163–181.
Calabresi, P., Centonze, D., Gubellini, P., Pisani, A., Bernardi, G., 1998. Endogenous ACh enhances striatal NMDA-responses via M1-like muscarinic receptors and PKC activation. Eur. J. Neurosci. 10, 2887–2895.
Dalley, J.W., Cardinal, R.N., Robbins, T.W., 2004. Prefrontal executive and cognitive functions in rodents: neural and neurochemical substrates. Neurosci. Biobehav. Rev. 28, 771–784.
Del Arco, A., Mora, F., 2009. Neurotransmitters and prefrontal cortex-limbic system interactions: implications for plasticity and psychiatric disorders. J. Neural Transm. 116, 941–952.
Dickinson, B.A., Jo, J., Seok, H., Son, G.H., Whitcomb, D.J., Davies, C.H., Sheng, M., Collingridge, G.L., Cho, K., 2009. A novel mechanism of hippocampal LTD involving muscarinic receptor-triggered interactions between AMPARs, GRIP and liprin-alpha. Mol. Brain 2, 18.
Feldman, D.E., 2009. Synaptic mechanisms for plasticity in neocortex. Annu. Rev. Neurosci. 32, 33–55.
Floresco, S.B., Seamans, J.K., Phillips, A.G., 1997. Selective roles for hippocampal, prefrontal cortical, and ventral striatal circuits in radial-arm maze tasks with or without a delay. J. Neurosci. 17, 1880–1890.
Garcia, R., Spennato, G., Nilsson-Todd, L., Moreau, J.L., Deschaux, O., 2008. Hippocampal low-frequency stimulation and chronic mild stress similarly disrupt fear extinction memory in rats. Neurobiol. Learn. Mem. 89, 560–566.
Goldman-Rakic, P.S., 1995a. Architecture of the prefrontal cortex and the central executive. Ann. N. Y Acad. Sci. 769, 71–83.
Goldman-Rakic, P.S., 1995b. Cellular basis of working memory. Neuron 14, 477–485.
Goto, Y., Yang, C.R., Otani, S., 2010. Functional and dysfunctional synaptic plasticity in prefrontal cortex: roles in psychiatric disorders. Biol. Psychiatry 67, 199–207.
Griffiths, S., Scott, H., Glover, C., Bienemann, A., Ghorbel, M.T., Uney, J., Brown, M.W., Warburton, E.C., Bashir, Z.I., 2008. Expression of long-term depression underlies visual recognition memory. Neuron 58, 186–194.
Groenewegen, H.J., Wright, C.I., Uylings, H.B., 1997. The anatomical relationships of the prefrontal cortex with limbic structures and the basal ganglia. J. Psychopharmacol. 11, 99–106.
Gu, Q., 2003. Contribution of acetylcholine to visual cortex plasticity. Neurobiol. Learn. Mem. 80, 291–301.
Gurden, H., Takita, M., Jay, T.M., 2000. Essential role of D1 but not D2 receptors in the NMDA receptor-dependent long-term potentiation at hippocampal-prefrontal cortex synapses in vivo. J. Neurosci. 20, RC106.
Hasselmo, M.E., 2006. The role of acetylcholine in learning and memory. Curr. Opin. Neurobiol. 16, 710–715.
Huang, C.C., Hsu, K.S., 2008. The role of NMDA receptors in regulating group II metabotropic glutamate receptor-mediated long-term depression in rat medial prefrontal cortex. Neuropharmacology 54, 1071–1078.
Huang, C.C., Hsu, K.S., 2010. Activation of muscarinic acetylcholine receptors induces a nitric oxide-dependent long-term depression in rat medial prefrontal cortex. Cereb. Cortex 20, 982–996.
Huerta, P.T., Lisman, J.E., 1995. Bidirectional synaptic plasticity induced by a single burst during cholinergic theta oscillation in CA1 in vitro. Neuron 15, 1053–1063.
Hyman, J.M., Zilli, E.A., Paley, A.M., Hasselmo, M.E., 2005. Medial prefrontal cortex cells show dynamic modulation with the hippocampal theta rhythm dependent on behavior. Hippocampus 15, 739–749.
Jay, T.M., Burette, F., Laroche, S., 1995. NMDA receptor-dependent long-term potentiation in the hippocampal afferent fibre system to the prefrontal cortex in the rat. Eur. J. Neurosci. 7, 247–250.
Jay, T.M., Glowinski, J., Thierry, A.M., 1989. Selectivity of the hippocampal projection to the prelimbic area of the prefrontal cortex in the rat. Brain Res. 505, 337–340.
Jay, T.M., Rocher, C., Hotte, M., Naudon, L., Gurden, H., Spedding, M., 2004. Plasticity at hippocampal to prefrontal cortex synapses is impaired by loss of dopamine and stress: importance for psychiatric diseases. Neurotox. Res. 6, 233–244.
Jay, T.M., Thierry, A.M., Wiklund, L., Glowinski, J., 1992. Excitatory amino acid pathway from the hippocampus to the prefrontal cortex. Contribution of AMPA receptors in hippocampo-prefrontal cortex transmission. Eur. J. Neurosci. 4, 1285–1295.
Jones, M.W., French, P.J., Bliss, T.V., Rosenblum, K., 1999. Molecular mechanisms of long-term potentiation in the insular cortex in vivo. J. Neurosci. 19, RC36.
Kemp, A., Manahan-Vaughan, D., 2007. Hippocampal long-term depression: master or minion in declarative memory processes? Trends Neurosci. 30, 111–118.
Kirkwood, A., Rozas, C., Kirkwood, J., Perez, F., Bear, M.F., 1999. Modulation of long-term synaptic depression in visual cortex by acetylcholine and norepinephrine. J. Neurosci. 19, 1599–1609.
Kruse, M.S., Premont, J., Krebs, M.O., Jay, T.M., 2009. Interaction of dopamine D1 with NMDA NR1 receptors in rat prefrontal cortex. Eur. Neuropsychopharmacol. 19, 296–304.
Laroche, S., Davis, S., Jay, T.M., 2000. Plasticity at hippocampal to prefrontal cortex synapses: dual roles in working memory and consolidation. Hippocampus 10, 438–446.
Laroche, S., Jay, T.M., Thierry, A.M., 1990. Long-term potentiation in the prefrontal cortex following stimulation of the hippocampal CA1/subicular region. Neurosci. Lett. 114, 184–190.
Lee, M.G., Chrobak, J.J., Sik, A., Wiley, R.G., Buzsaki, G., 1994. Hippocampal theta activity following selective lesion of the septal cholinergic system. Neuroscience 62, 1033–1047.
Leite, J.P., Bortolotto, Z.A., Cavalheiro, E.A., 1990. Spontaneous recurrent seizures in rats: an experimental model of partial epilepsy. Neurosci. Biobehav. Rev. 14, 511–517.
Leite, J.P., Garcia-Cairasco, N., Cavalheiro, E.A., 2002. New insights from the use of pilocarpine and kainate models. Epilepsy Res. 50, 93–103.
Lopes Aguiar, C., Romcy-Pereira, R.N., Escorsim Szawka, R., Galvis-Alonso, O.Y., Anselmo-Franci, J.A., Pereira Leite, J., 2008. Muscarinic acetylcholine neurotransmission enhances the late-phase of long-term potentiation in the hippocampal-prefrontal cortex pathway of rats in vivo: a possible involvement of monoaminergic systems. Neuroscience 153, 1309–1319.
Lucas-Meunier, E., Fossier, P., Baux, G., Amar, M., 2003. Cholinergic modulation of the cortical neuronal network. Pflugers Arch. 446, 17–29.
Martin, S.J., Morris, R.G., 2002. New life in an old idea: the synaptic plasticity and memory hypothesis revisited. Hippocampus 12, 609–636.
Marzo, A., Bai, J., Caboche, J., Vanhoutte, P., Otani, S., 2010. Cellular mechanisms of long-term depression induced by noradrenaline in rat prefrontal neurons. Neuroscience 169, 74–86.
Massey, P.V., Bashir, Z.I., 2007. Long-term depression: multiple forms and implications for brain function. Trends Neurosci. 30, 176–184.
Matsuda, Y., Marzo, A., Otani, S., 2006. The presence of background dopamine signal converts long-term synaptic depression to potentiation in rat prefrontal cortex. J. Neurosci. 26, 4803–4810.
McCoy, P.A., McMahon, L.L., 2007. Muscarinic receptor dependent long-term depression in rat visual cortex is PKC independent but requires ERK1/2 activation and protein synthesis. J. Neurophysiol. 98, 1862–1870.
Ohashi, S., Matsumoto, M., Togashi, H., Ueno, K., Yoshioka, M., 2003. The serotonergic modulation of synaptic plasticity in the rat hippocampo-medial prefrontal cortex pathway. Neurosci. Lett. 342, 179–182.
Otani, S., 2003. Prefrontal cortex function, quasi-physiological stimuli, and synaptic plasticity. J. Physiol. Paris 97, 423–430.
Paxinos, G., Watson, C., 2007. The Rat Brain in Stereotaxic Coordinates. Academic Press/Elsevier, Amsterdam, Boston.
Raedler, T.J., Bymaster, F.P., Tandon, R., Copolov, D., Dean, B., 2007. Towards a muscarinic hypothesis of schizophrenia. Mol. Psychiatry 12, 232–246.
Rocher, C., Spedding, M., Munoz, C., Jay, T.M., 2004. Acute stress-induced changes in hippocampal/prefrontal circuits in rats: effects of antidepressants. Cereb. Cortex 14, 224–229.
Romcy-Pereira, R., Pavlides, C., 2004. Distinct modulatory effects of sleep on the maintenance of hippocampal and medial prefrontal cortex LTP. Eur. J. Neurosci. 20, 3453–3462.
Romcy-Pereira, R.N., Erraji-Benchekroun, L., Smyrniotopoulos, P., Ogawa, S., Mello, C.V., Sibille, E., Pavlides, C., 2009. Sleep-dependent gene expression in the hippocampus and prefrontal cortex following long-term potentiation. Physiol. Behav. 98, 44–52.
Scarr, E., Dean, B., 2008. Muscarinic receptors: do they have a role in the pathology and treatment of schizophrenia? J. Neurochem. 107, 1188–1195.
Seidenbecher, T., Laxmi, T.R., Stork, O., Pape, H.C., 2003. Amygdalar and hippocampal theta rhythm synchronization during fear memory retrieval. Science 301, 846–850.
Siapas, A.G., Lubenov, E.V., Wilson, M.A., 2005. Prefrontal phase locking to hippocampal theta oscillations. Neuron 46, 141–151.
Swanson, L.W., 1981. A direct projection from Ammon's horn to prefrontal cortex in the rat. Brain Res. 217, 150–154.
Takita, M., Izaki, Y., Jay, T.M., Kaneko, H., Suzuki, S.S., 1999. Induction of stable long-term depression in vivo in the hippocampal-prefrontal cortex pathway. Eur. J. Neurosci. 11, 4145–4148.
Thierry, A.M., Gioanni, Y., Degenetais, E., Glowinski, J., 2000. Hippocampo-prefrontal cortex pathway: anatomical and electrophysiological characteristics. Hippocampus 10, 411–419.
Uylings, H.B., Groenewegen, H.J., Kolb, B., 2003. Do rats have a prefrontal cortex? Behav. Brain Res. 146, 3–17.
Vertes, R.P., 2006. Interactions among the medial prefrontal cortex, hippocampus and midline thalamus in emotional and cognitive processing in the rat. Neuroscience 142, 1–20.
Wang, L., Yuan, L.L., 2009. Activation of M2 muscarinic receptors leads to sustained suppression of hippocampal transmission in the medial prefrontal cortex. J. Physiol. 587, 5139–5147.
Warburton, E.C., Koder, T., Cho, K., Massey, P.V., Duguid, G., Barker, G.R., Aggleton, J.P., Bashir, Z.I., Brown, M.W., 2003. Cholinergic neurotransmission is essential for perirhinal cortical plasticity and recognition memory. Neuron 38, 987–996.
Wierzynski, C.M., Lubenov, E.V., Gu, M., Siapas, A.G., 2009. State-dependent spike-timing relationships between hippocampal and prefrontal circuits during sleep. Neuron 61, 587–596.
Winocur, G., Moscovitch, M., Bontempi, B., 2010. Memory formation and long-term retention in humans and animals: convergence towards a transformation account of hippocampal-neocortical interactions. Neuropsychologia 48, 2339–2356.
Yun, S.H., Cheong, M.Y., Mook-Jung, I., Huh, K., Lee, C., Jung, M.W., 2000. Cholinergic modulation of synaptic transmission and plasticity in entorhinal cortex and hippocampus of the rat. Neuroscience 97, 671–676.
Zhang, Z.W., Burke, M.W., Calakos, N., Beaulieu, J.M., Vaucher, E., 2010. Confocal analysis of cholinergic and dopaminergic inputs onto pyramidal cells in the prefrontal cortex of rodents. Front. Neuroanat. 4, 21.
Zhao, Y., Tzounopoulos, T., 2011. Physiological activation of cholinergic inputs controls associative synaptic plasticity via modulation of endocannabinoid signaling. J. Neurosci. 31, 3158–3168.